Int. J. Nonlinear Anal. Appl. 13 (2022) 2, 1053–1067
ISSN: 2008-6822 (electronic)
http://dx.doi.org/10.22075/ijnaa.2022.6366

# MIMO access point and practical challenges in DAS over RoF-OFDM systems

Musaddak M. Abdul Zahra[a,b,*], Laith A. Abdul-Rahaim[a], Aqeel H. Al-fatlawi[c], Yazen S. Almashhadani[d], Hawraa N. Jasim[b]

[a] *Electrical Engineering Department, College of Engineering, University of Babylon, Babylon, Iraq*

[b] *Computer Techniques Engineering Department, Al-Mustaqbal University College, Babylon 51001, Iraq*

[c] *Department of Computer Techniques, Imam Kadhum College, Iraq*

[d] *Department of Communication and Computer Engineering, Cihan University-Erbil, Kurdistan Region, Iraq*

*(Communicated by Javad Vahidi)*

**Abstract**

The use of commercial MIMO APs in RoF-DAS results in substantial throughput reduction. Efficient use of multi-antenna scheme algorithms allows for significant physical separation between the radio units, which results in decreased error rates and increased capacity. MIMO wireless communications in a DAS, which utilizes RoF to increase the overall wireless coverage and capacity have been the focus of this thesis. The main goal is to explore the factors that contribute to throughput declines in an RFDAS when commercial MIMO APs are utilized. Practical challenges are considered to examine the RoF-DAS. Single and multiple-use experience is taken for finding the experimental setup. The investigation revealed that the amount of data the system can transmit correlates with the imbalance in the received power, and the imbalance in the received power correlates with the amount of data the system can transmit.

Keywords: MIMO, APs, RFDAS, RoF-DAS, fiber length
2020 MSC: 90B10, 91D10

## 1 Introduction

In contrast to relay and femtocell networks, a DAS system is used to distribute a mobile phone signal. In order to provide a wide wireless coverage area for interior clients, these radio-over-fibre (RoF) links, coaxial cables, or out-of-band radio links connect the base stations to the building. Since delivering excellent signal coverage while maintaining a high signal-to-noise ratio, DAS has been getting a lot of attention in-building scenarios [14]. Using DAS to launch new wireless services, like advanced modulation, OFDM, sophisticated coding, and MIMO, is also made easier because everything takes place in one spot.

The central unit (CU) is home to the base station equipment and wireless access points (WAPs). To meet the requirements of ROAUs, the CU connects to the ROAUs via ROF links. It is possible to link the CU to the RAUs via coaxial cable, but because of the relatively high attenuation of this type of cable, the CU and the RAUs cannot be placed much further apart without significant attenuation. Distributed antennas carry execute the signal processing at the CU, such as modulation, demodulation, and multiplexing.

*Corresponding author
*Email addresses:* musaddaqmahir@mustaqbal-college.edu.iq (Musaddak M. Abdul Zahra ), aqeelhamah@alkadhum-col.edu.iq (Aqeel H. Al-fatlawi)

*Received:* November 2021 *Accepted:* February 2022

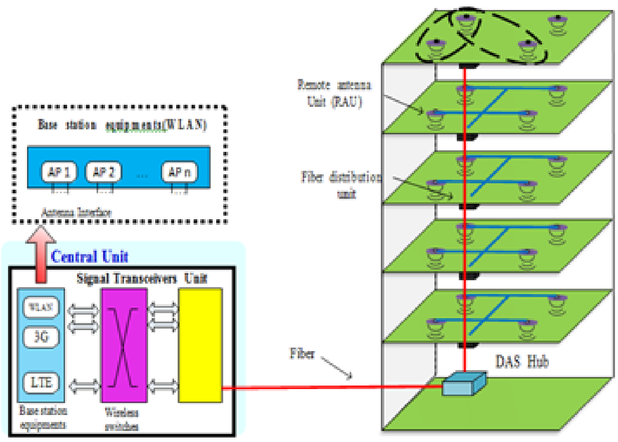


Figure 1: RoF-based DAS

## 2 Distributed Antenna System (DAS) deployed In-building

In order to boost wireless coverage in buildings, more APs are required.

**RoF Link configurations**

The flow rate link in figure 2 is depicted as being part of a larger RF system.

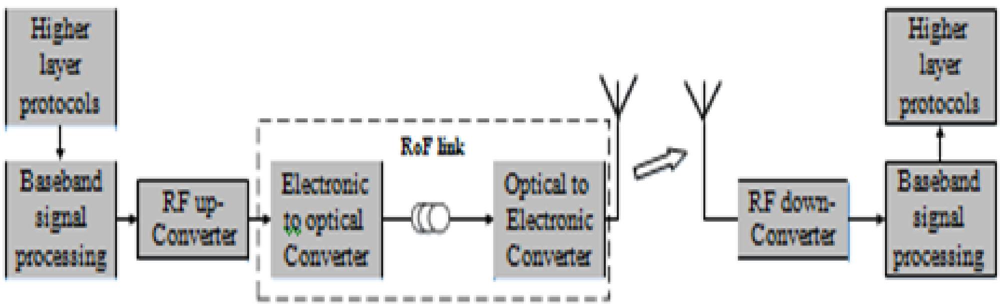


Figure 2: RoF Link

The baseband does the work of signal processing like modulation and coding. It is converted from an optical signal to an electrical signal at the receiving end before the signal from the baseband is sent via the wireless connection. After being received by the receiver unit, the RF signal is down-converted and passed to baseband protocols for further processing. RoF connection topologies consist of varying combinations of fiber-to-fiber links and fiber-to-signal fiber links. This type of arrangement is known as a fiber-to-fiber link since it uses fiber-optic cable to send the optical signal through to a PD receiver[7]. After it has been successfully sent, the recovered RF signal is amplified by the PD and sent out wirelessly.

## 3 MIMO System

Moving from 802.11b to 802.11g involved introducing OFDM, which improved the ability to combat frequency selective fading. Prior to the introduction of the MIMO system in the IEEE 802.11n standard, the IEEE 802.11a/b/g compliant APs used the SISO system to transmit and receive RF signals, but the IEEE 802.11n standard incorporated the MIMO system for improved data rates and signal quality to keep pace with the demand for fast networks[1, 3, 2, 12].

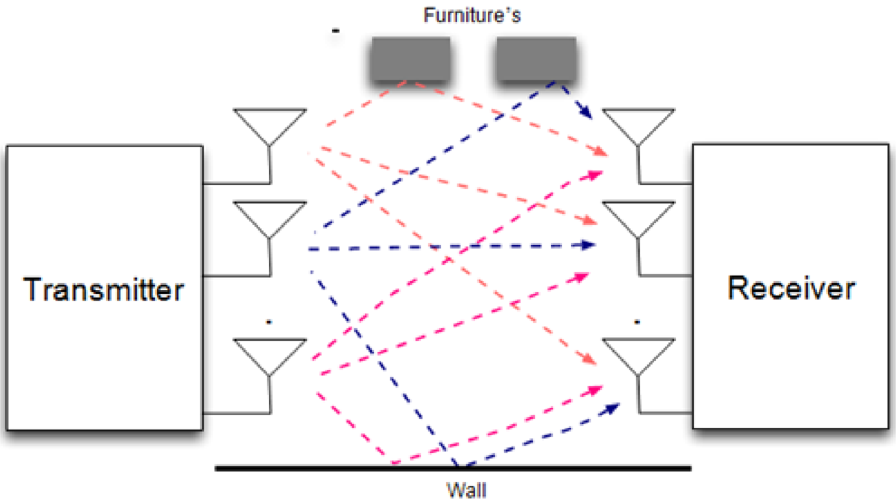


Figure 3: Multipath fading for MIMO.

A multihued multipath propagation channel may be used to send and receive signals from multihued antennas, as shown in figure 3. DSP technology extracts the original signals from the antennas, and then transmits them. IEEE 802.11n supports three spatial streams (33 MIMO) and a maximum channel bandwidth of 40MHz. Only a few chips and APs handle the many spatial streams found in IEEE 802.11n. 802.11ac protocol WLAN equipment has lately seen an upsurge in shipments, incorporating the prior 802.11n standard, but with faster data transfer speeds of up to 1.3Gbps.

Spatial diversity technique is used to improve the radio link dependability also this special multiplexing is very useful to improve the data speed. Construction of 802.11n-enabled wireless networks requires the use of both spatial diversity and spatial multiplexing. When the signal-to-noise ratio is high, APs can use multiple spatial diversity and multiple spatial multiplexing techniques (SNR)[5]. Spatial multiplexing, spatial diversity, or SISO may be automatically used if the signal quality is good. Transmit Beam Focusing (TxBF) is an optional feature of the IEEE 802.11ac standard, sometimes referred to as Wi-Fi 6.

**MIMO Performance in RoF-DAS**

Due to its centralized architecture, DASs are capable of improving overall system performance by enabling collaborative processing activities like effective resource allocation, co-channel interference cancellation, and signal delay management. By using DAS, it is possible to integrate more services easily while implementing the newest, most modern wireless service standards, such as OFDM, MIMO, and OFDM[8].

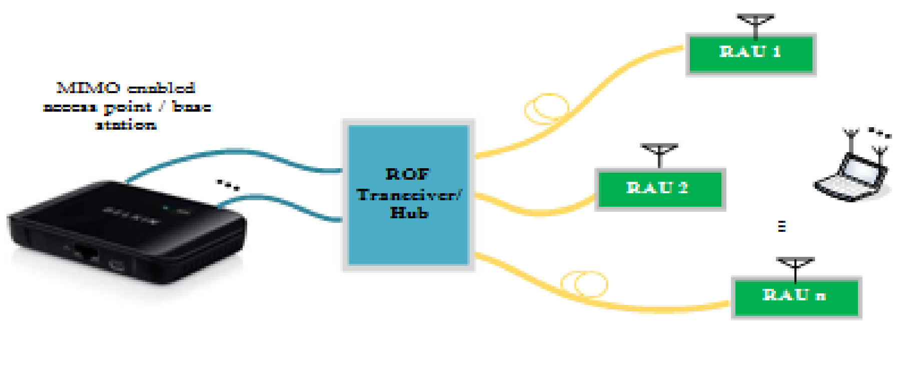


Figure 4: A 2x2 MIMO over RoF DAS diagram.

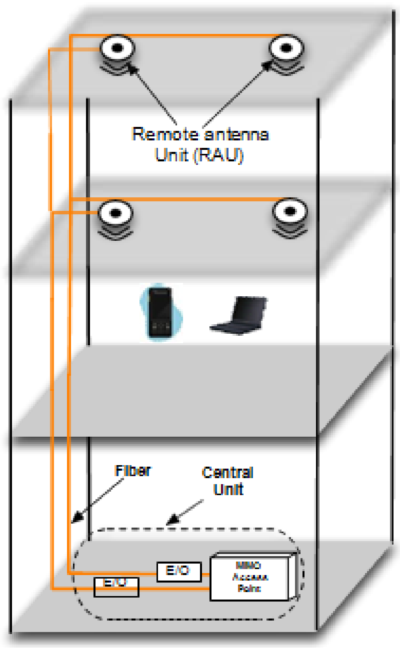


Figure 5: 2x2 MIMO AP in RoF-DAS

This will result in a further improvement in the overall system performance due to the increased channel decorrelation brought on by MIMO and RoF-DAS integration. To work with MIMO, both the wireless user and the transmission system must have very high signal-to-noise ratios, such as 16-QAM and 64-QAM. Having RoF-DAS on-board allows for a broad MIMO antenna spacing, which leads to larger spatial decorrelation and improved SNR. An IEEE 802.11n/ac-compatible WLAN AP such as the one illustrated in figure 5 can easily be accommodated in the RoF-DAS architecture.

## 4 Practical and commercial MIMO network access points are featured in DAS

This technology is also supported in the MIMO DAS protocol. There have been reports on RoF-DAS MIMO throughput and capacity that have not mentioned real-world difficulties that could slow down MIMO signal transmission over the infrastructure [3]. To optimize the system performance, DAS operators must compensate for these challenges. This research begins by taking into consideration two important concerns for network designers, including MIMO and RoF-DAS, followed by the relevant measurement findings and a conclusion.

**Practical challenges relating to MIMO-DAS**

Past research has shown that distributing WLAN signals over DAS results in considerable throughput reductions due to changes in fiber lengths between the campus units and the roaming areas, which leads to wasteful usage of DAS. A longer delay spread results from the DAS's amplification and preservation of the signal paths that lead to every RAALU. The inter-symbol interference (ISI) results from this (ISI). When the distance to the wireless receiver grows, the throughput halves. IEEE 802.11g sets rigorous SNR and delay spread requirements, which leads in data speeds doubling. As a result, the AP transmits data at a lower data rate under worst-case propagation conditions. [13] Prior works have primarily utilized non-MIMO APs for analyzing the influence of fiber length on DAS.

A single RF chain is not sufficient for MIMO; in addition, multiple RF chains are necessary in a RoF-DAS deployment since each RF chain from the CU to the RAUs is connected to each RAU. In order to increase signal quality and data throughput, the signals from the UE should be aligned prior to joining. Because of a big fibre link differential, it's difficult to get a signal, and so ISI has increased significantly. Other systems, in order to achieve spatial separation of the wireless channels, require at least $\frac{1}{4}$ of a radio signal wavelength of space between antennas. Using optical feed of the antennas, it is possible to space the antennas substantially farther apart, which enables the use of MIMO in covering bigger regions [10].

In order to improve the throughput performance, increasing the distance between each of the relevant Resource

Allocation Units (RAUs) helps improve the wireless coverage. A receiver power imbalance that decreases throughput performance could also result from an antenna separation distance that is too great. MIMO's difficulty is that the two received signals' intensities are not equal. In the MIMO-DAS system, power levels will be consistent over an entire facility, but in a realistic scenario with high antenna separation, this is not necessarily the case[6]. Thus, it's important to consider both the reduction of correlation and the diminishment of the received power imbalance when deploying MIMO-DAS.

This research analyses throughput utilising two alternative IEEE 802.11n 2x2 MIMO APs with various fibre lengths and power imbalances in a RoF-based DAS. One examination of fiber length discrepancy examines seven different situations for MIMO-assisted APs, five of which have MIMO assistance, and two for spatial diversity-assisted APs. To learn more about throughput in the presence of wireless users, the experiment used a typical office environment as a reference. The change in fiber length ranged from 25m to 150m. An analysis that uses MIMO- and spatial-diversity-supported APs may be utilized to calculate the amount of power available for different setups.[17] Despite the room's insufficient size, power imbalance induced route losses were nevertheless measured because we generated them utilizing the use of various power levels at each ROU. Before the antennas were employed in the experiment, the output power levels were changed such that the UE would face high power imbalances. This has contributed to the large imbalance visible in the experiment.

## 5 Experimental Setup

In figure 6, you can see an experimental configuration that demonstrates bi-directional MIMO-over-fiber DAS. An Ethernet connection with a data transfer rate of 1 gigabit was used to link the AP to a host PC. MIMO-enabled Single-mode fibre (SMF) cables are used to deliver the generated optical signals to the Remote Area Units.[16] To get optical signals to the photodiodes, photodiodes were used to detect the optical signals, which were then amplified by an electrical amplifier for transmission through the wireless route.

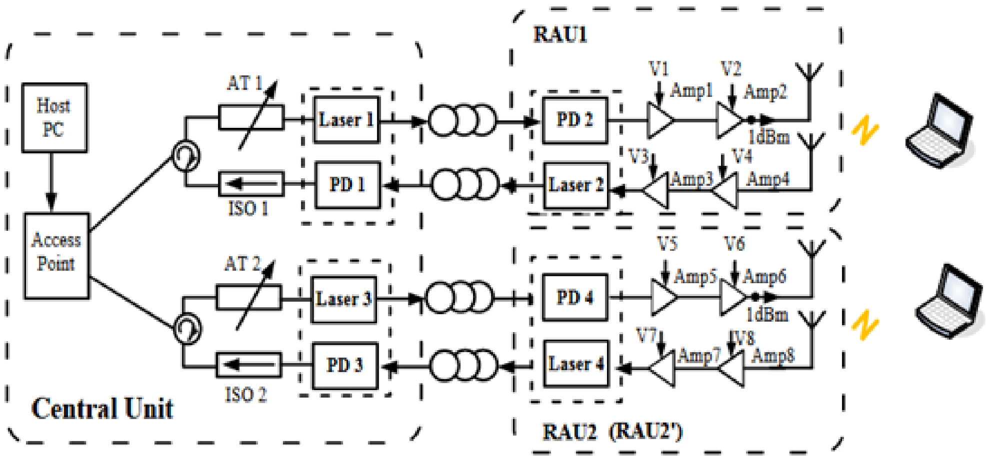


Figure 6: (a) The experiment set-up.

This includes a host computer, a downlink LD, an uplink PD, and other equipment, such as PCs, chairs, and desks. While placing the RAUs on a wooden platform, it was often the case that the signals were radiated over any furniture. In figure 8, the example of the testing room, A, B, C, shows rows and columns to illustrate where measurements were made on the UE. The RF signals were amplified and then up-converted at the RAUs before being transformed into optical signals. In order to do this, the signals were first converted to an intermediate frequency (IF) signal. [11, 15, 4].Once the signals had been sent along the SMF line segments, they were transformed to an RF signal at the CU where the signals were applied to the final target devices. Once the PDs were in place, RF isolators were employed to route signals in only one direction. The output power of each antenna was set to 1 dBm, and the amplifiers were tested to see if the cascaded amplifiers were working in their linear zone. This particular type of antenna, known as an antenna parabola, was employed in the studies and its total gain is roughly 9.5 dBi.

Table 1: Parameters used in the testing

| AP Type | Parameter | Value |
|---|---|---|
| **Spatial diversity-supported AP Experiment** | Antenna Gain | 9.5dBi |
| | Bandwidth | 20MHz |
| | Measured Date Rate | 25Mbps |
| | Modulation | OFDM |
| | RAU Transmit Power | 1dBm |
| | Band of RF | 2.4 GHz |
| | RoF Link Gain | -25dB |
| **Experiment of MIMO-based AP** | Measured Date Rate | 96Mbps |
| | RAU Transmit Power | 1dBm |
| | Band of RF | 2.0 to 2.4 GHz |
| | RoF Link Gain | -25dB |
| | Bandwidth | 20/40MHz auto |
| | Antenna Gain | 9.5dBi |
| | Modulation | OFDM-MIMO |

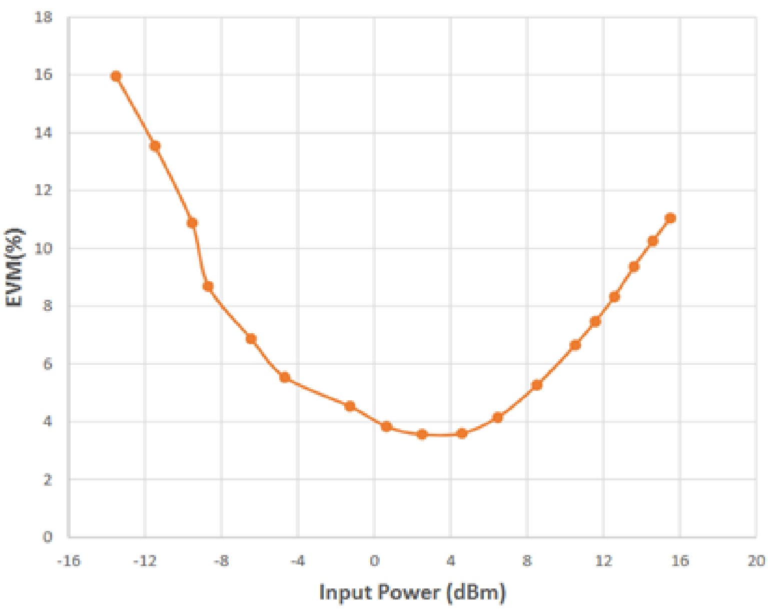


Figure 7: Laser diode coupled to a photodiode's input power (PD)

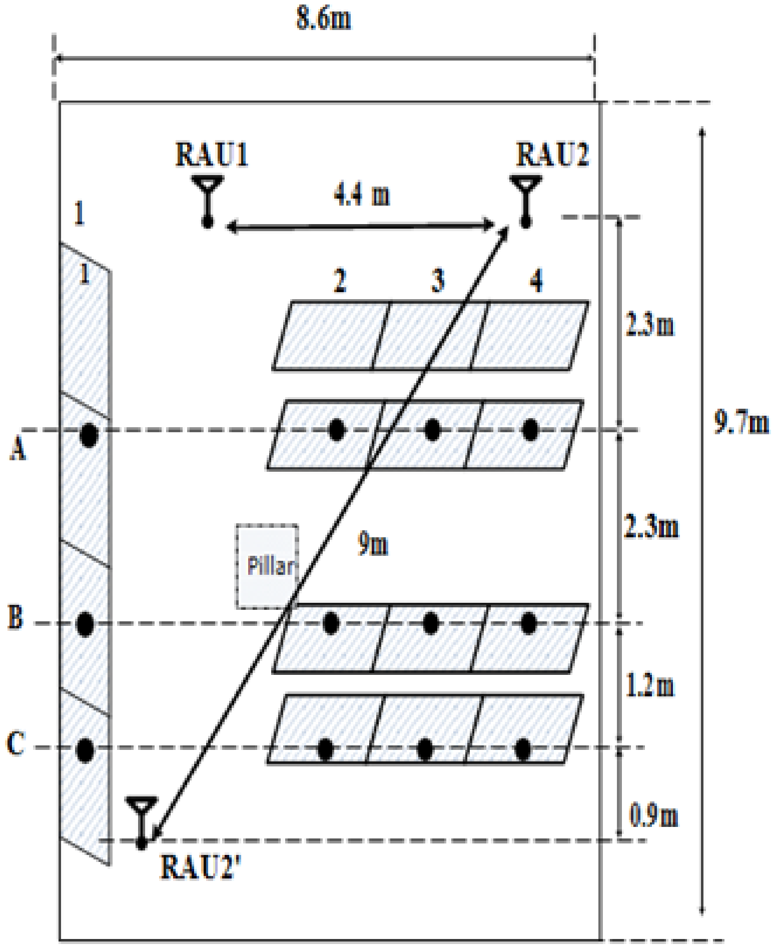


Figure 8: Experiment layout.

An EVM measurement was done to arrive at the optimal input power to the RoF link. The resulting signal was put into a vector signal generator created using an Agilent WLAN software (VSG). A laptop with Agilent demodulation software was used to demodulate the signal after it was delivered across the RoF link (VSA).

The separation distance was modified to 4.4m and 9m in the testing room, in order to conduct an analysis of the throughput between the two antenna separations. Spatial correlation is reduced, causing increased RF strength for all of the cell's UEs, especially those which are closest to the base stations. A significant number of files were copied between the host PC and laptops, mobile, allowing throughput tests to be conducted. These large black dots represent where mobile devices are situated in the illustration above.

**Fiber length difference analysis results**

From the diagram above, it can be seen that the two testing rooms are separated by a distance of 4.4 meters, which means that the CU and the RAUs are to be located behind the testing room. It is important to note that although the output power was the same, the operating temperature for each unit was different. We do this to investigate the throughput performance in the RoF-DAS with varying fibre length differences between the APs that are both MIMO-supported and those that offer spatial diversity.[12, 9] Seven experiments were conducted with seven distinct setups, as seen in table 2. figure 8 shows the measured throughputs in each user position for the tests in Case 1 through Case 7. In examples 1 through 5 on the campus, a 1.2 GHz Cisco Aironet adapter with a Cisco 802.11n MIMO radio is used, whereas in cases 6 and 7, a 3Com 3D spatial diversity adapter is employed.

**Measurements for Single user**

The downlink throughput is shown in figure 9 to 11, and these measurements are normalized to represent the highest possible throughput. It was tested in a laboratory before being connected to the RoF lines. The highest

Table 2: System configurations for calculating fiber length differences

| | Access Point Type | Fiber Length-RAU1(m) | Fiber Length-RAU2(m) |
|---|---|---|---|
| $1^{st}$ case | Multiple Input Multiple Output | 25 | 25 |
| $2^{nd}$ case | | 75 | 25 |
| $3^{rd}$ case | | 125 | 25 |
| $4^{th}$ case | | 175 | 25 |
| $5^{th}$ case | | 125 | 125 |
| $6^{th}$ case | Spatial Diversity | 25 | 25 |
| $7^{th}$ case | | 175 | 25 |

throughput that can be reached by the AP using spatial diversity is 25Mbps, however, when MIMO is in use, the highest throughput that can be achieved is 96Mbps, as it is twice the bandwidth of the AP that relies on spatial diversity.

In all three of these scenarios, the throughput decreases steadily as the difference in fiber length increases. Increasing the fiber length difference causes the ISI to introduce a longer delay, which lengthens the separation of the two RAUs' received signals. This confirms that when it was determined that the fiber link difference (directivity) increases when it exceeds a particular distance, which causes the differential latency to increase, resulting in reduced throughput. Case 1's normalized throughput performance was practically the same for all tested places due to the equal number of fiber links.

Because in this case both RAUs (RAU1 and RAU2) had identical lengths but had more fibre, the throughput is not substantially affected (in comparison to Case 5, where only one RAU had comparable lengths) (compared to Case 5). Delays in getting responses. The rise in differential delay, which was not the result of a change in fixed fibre delay, is the reason why throughput has declined in figure 9.

figure 11 illustrates the output of geographic diversity AP throughput measurement. Only one antenna port is in use in this AP. Because the normalized throughput barely changed in Case 6 to Case 7, it may be deduced that. The system performance does not suffer as long as only the antenna that is receiving higher power or SNR is picked.

**Multiple user measurements**

Additionally, to assess the impact of having several users connecting to the AP from both antenna ports, an additional UE was installed. The number of Network Interface Cards (NIC) was evened out to provide an equal model to compare laptops.

Each manufacturer implements various MAC configurations, which can greatly affect the throughput distribution. This network design is designed to guarantee the greatest feasible bandwidth. In order to do this, not even 802.11b devices were detected inside the radius of the 802.11g wireless access point.

RAU1 and RAU2 were positioned at separate locations in the room for the multiple user experiment. G1 describes all three laptops having been positioned in column A, row 1. G2 describes both laptops being in column A, row 2. G3 describes the laptops being in rows B and 4, respectively. Finally, G4 describes one laptop in column A, row 1, and the other one in rows B and 4. After the speed of the two laptops reached a certain threshold, the data recording started at the same moment. The downlink and uplink normalized throughput performance of the 2-laptop situation is shown on figures 12 and 13. In a similar fashion, figure 12 and 13 show that, when a MIMO access point is used in the configuration of 25m-175m, normalized throughput for both uplink and downlink is considerably lower than in the 25m-25m configuration. While throughput for the most part remained normal when the diversity antenna was implemented, a small drop was detected since only one antenna is used at a time.

**Result Analysis for Power imbalance**

Since the test room was too small to accurately measure the route losses caused by antenna separation, the power imbalance effect was intentionally manufactured by adjusting the levels of transmitting power for all RAUs.

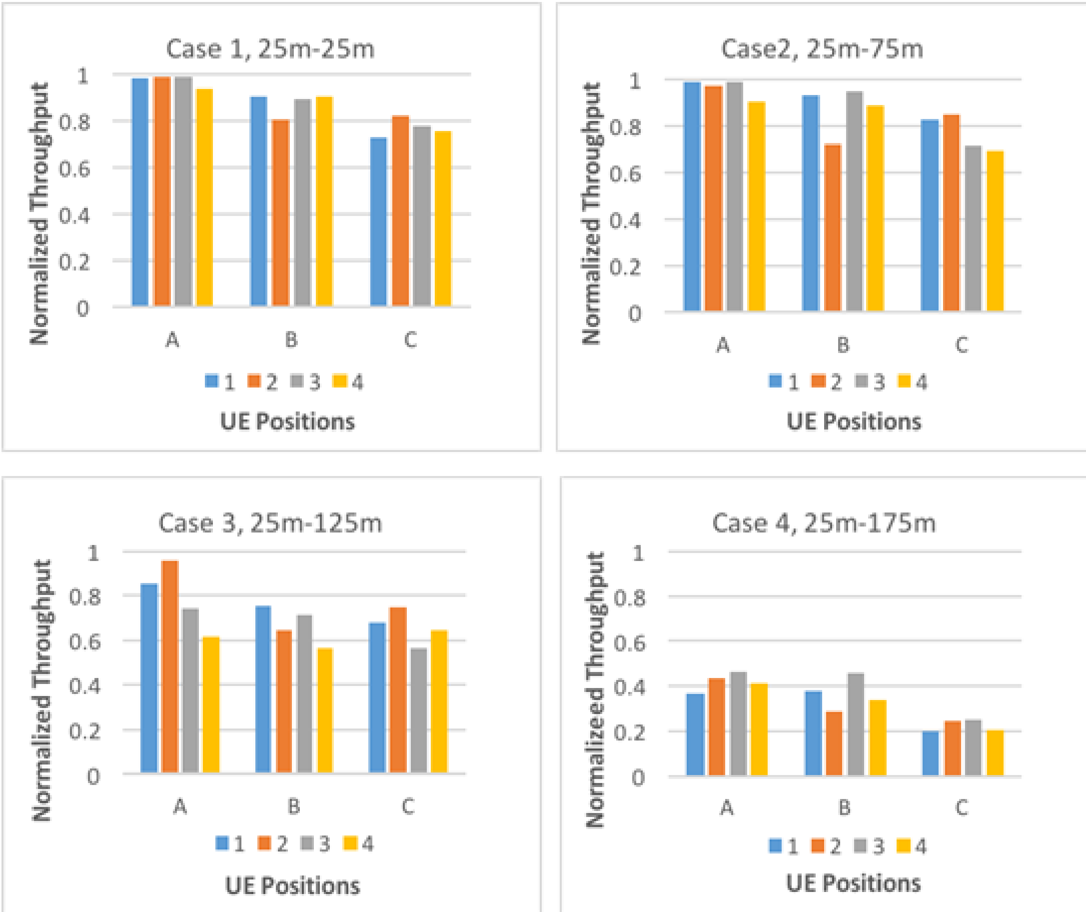


Figure 9: Different fiber lines supported in a MIMO-enabled downlink throughput

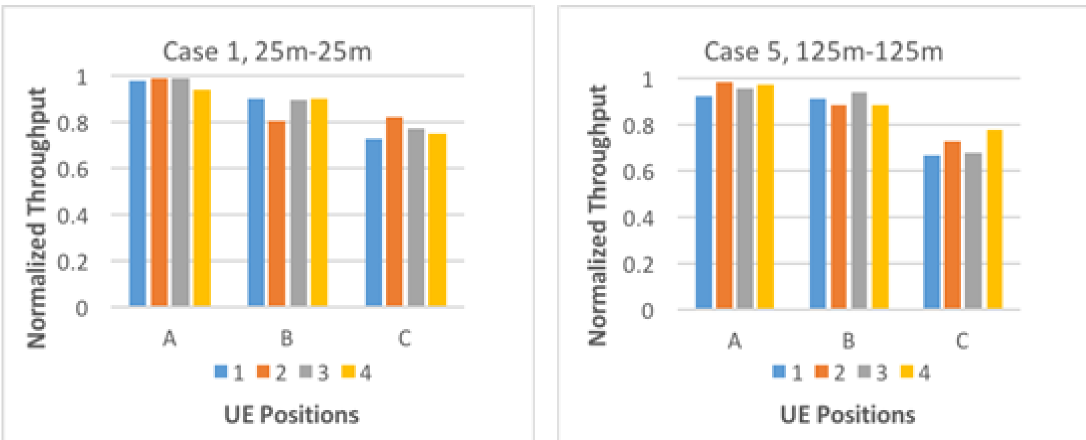


Figure 10: with the same fibre link lengths, MIMO-enabled downlink throughput

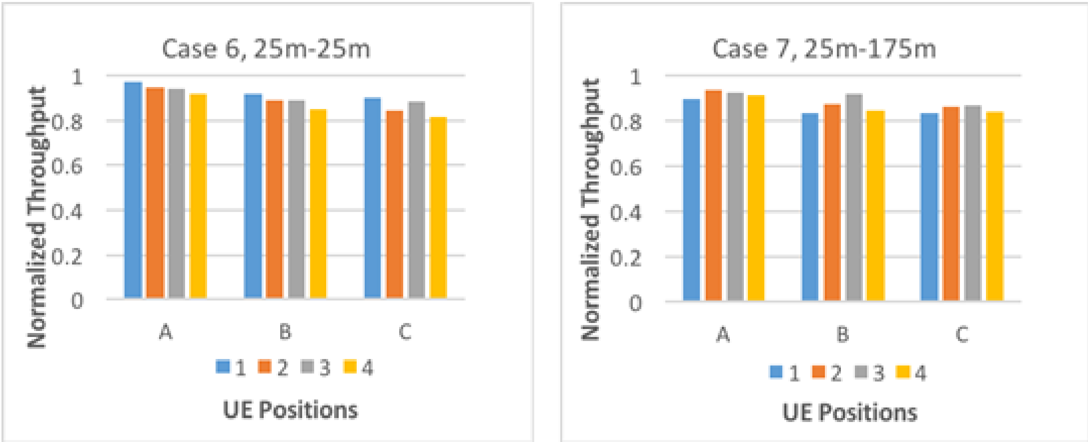


Figure 11: SD-supported down link output, where each link length of the fiber supports a distinct downstream throughput

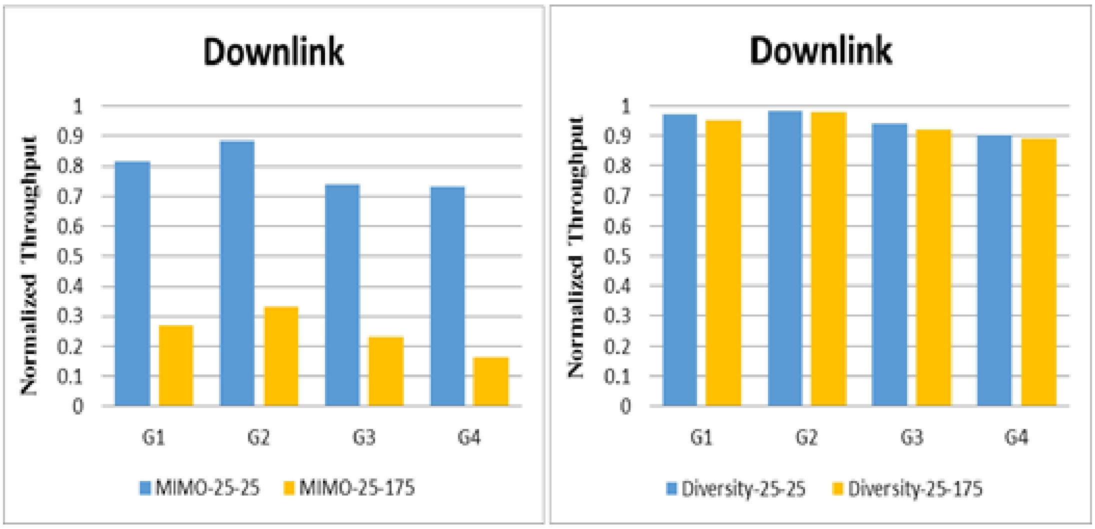


Figure 12: Fiber connections are compared to multiple users using MIMO and diversity antennae in terms of total downlink speed

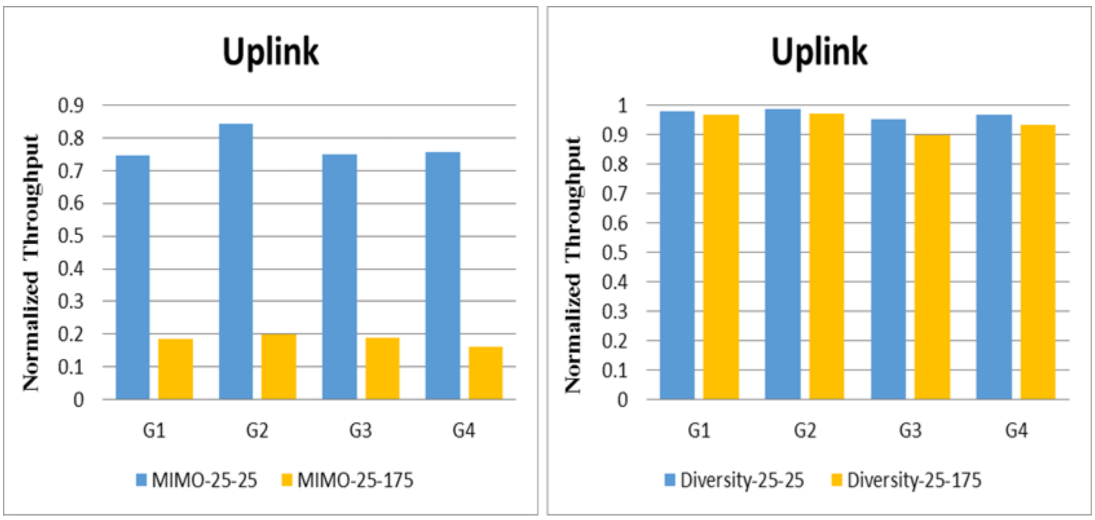


Figure 13: For Diversity AP and a MIMO AP, the uplink output can be measured multiple times and compared.

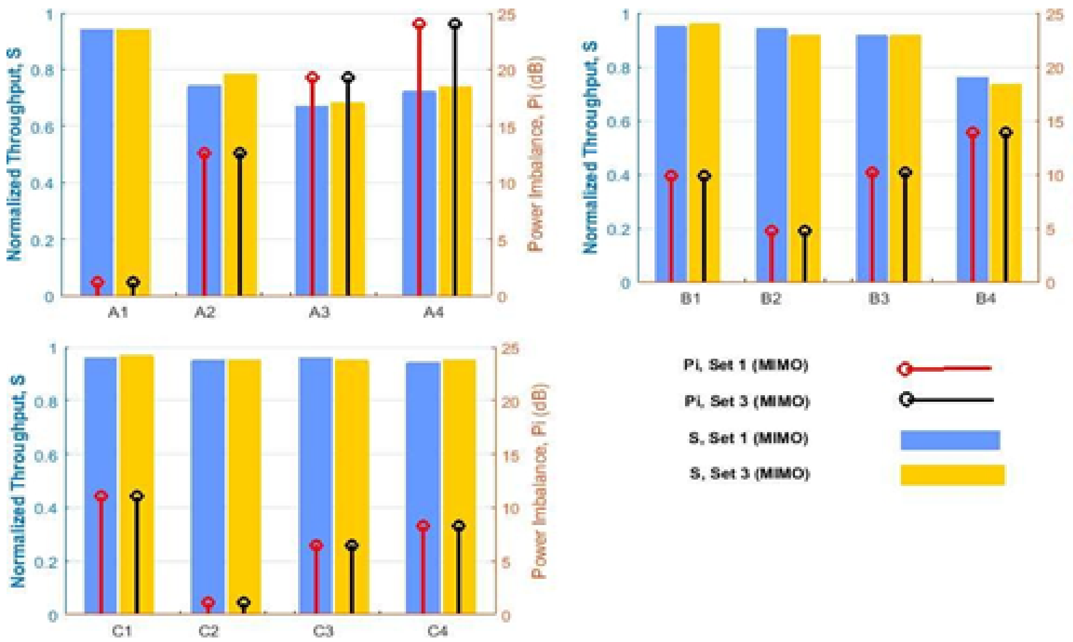


Figure 14: Throughputs S and unbalance in power Set 1 and set 3 results for MIMO with Pi

To get a desired output power for each antenna the resulting voltages were combined into sets. The antenna sets deliver different amounts of power with varying transmit power from each antenna. Set 1 (the larger antenna with three additional antenna pieces) has a higher output than set 3 (the smaller antenna with two additional antenna pieces). Set 2 (the smaller antenna with two additional antenna pieces) has a lower output than set 4 (the larger antenna with three additional antenna pieces). For Sets (5&6), the production of high value of power is uneven.

When doing the experiment, it's possible to see a higher received power imbalance because of the differences in output power and path loss.

$$L_{path}=20\times\log10(f) + N\times\log10(d) + Lf(n) - 28dB$$

Lf(n) is the floor penetration loss factor, and n is related to f, d, and Lf(n) by the formula: The denominator, which is the number of floors, is equal to zero.

After the model had been tested in the usual office area was calculated to have a value of N=28. In figures 14, 15, and 16, the MIMO-DAS throughput is shown to be inversely proportional to the received power imbalance when various combinations of sets are used. When computing Throughput and Power Imbalance, consider the number on the horizontal axis, S, and the number on the vertical axis, Pi (dB). The positions of a single user is described in figure 6 participated in the experiment, which took place with both RAUs (RAU 1 and RAU 2) at a distance of 9 meters apart in a room. Since they were 9 meters apart, RAU 2 was placed at the other end of the room. The points are situated far from (RAU1 and RAU2) than are in position (A1, B1, and C1). Each operational mode's maximum throughput has been applied to normalize performance.

Figure 14 illustrates the findings of sets (1&3), which have an imbalance power of 8.2dB, but each RAU has a different output power. It can be seen that power imbalance of 12dB or more reduces throughput.

- Throughput is indicated by S,
- Power received from RAU1 and RAU2 is indicated as Pr1 & Pr2
- Power Imbalance (dB) is indicated by Pi

Figure 16 depicts the performance comparison between MIMO-supported APs and spatial diversity-supported APs. A graph from figure 16 indicates that MIMO-supported AP performance gradually decreases the more apart the receiving antenna units . The diversity strategy avoids mixing the antenna signals, eliminating the power imbalance issue. Because of the antenna path chosen, the antenna with the most signal power is selected. It can be shown from figures 14 to 16 that throughput declines when the imbalance in power received surpasses 12dB. There is no drop in

Table 3: Experimental Results for Set3 & Set1

| | | Set 3 | | | | Set 1 | | | |
|---|---|---|---|---|---|---|---|---|---|
| | | 1 | 2 | 3 | 4 | 1 | 2 | 3 | 4 |
| Row A | S | 0.946 | 0.791 | 0.69 | 0.74 | 0.946 | 0.739 | 0.67 | 0.718 |
| | Pi (dB) | 1.09 | 12.59 | 19.31 | 23.98 | 1.12 | 12.71 | 19.31 | 24.06 |
| | Pr1(dBm) | -54.65 | -46.6 | -42.27 | -39.69 | -51.35 | -43.3 | -38.97 | -36.39 |
| | Pr2(dBm) | -55.71 | -59.29 | -61.51 | -63.87 | -52.49 | -55.89 | -58.21 | -60.39 |
| Row B | S | 0.958 | 0.916 | 0.916 | 0.734 | 0.92 | 0.96 | 0.91 | 0.78 |
| | Pi (dB) | -9.85 | 4.75 | 10.2 | 13.84 | -9.85 | 4.75 | 10.2 | 13.84 |
| | Pr1(dBm) | -56.1 | -50.98 | -49.13 | -48.49 | -52.82 | -47.56 | -45.83 | -45.12 |
| | Pr2(dBm) | -46.36 | -55.73 | -59.36 | -61.53 | -42.97 | -52.35 | -56.03 | -58.23 |
| Row C | S | 0.968 | 0.946 | 0.946 | 0.95 | 0.957 | 0.94 | 0.968 | 0.942 |
| | Pi (dB) | -11.12 | 1.08 | 6.41 | 8.31 | -11.05 | 1.09 | 6.49 | 8.33 |
| | Pr1(dBm) | -55.75 | -53.36 | -52.22 | -51.79 | -52.65 | -49.86 | -48.72 | -48.4 |
| | Pr2(dBm) | -44.81 | -54.73 | -58.53 | -59.22 | -41.45 | -51.01 | -55.23 | -55.72 |

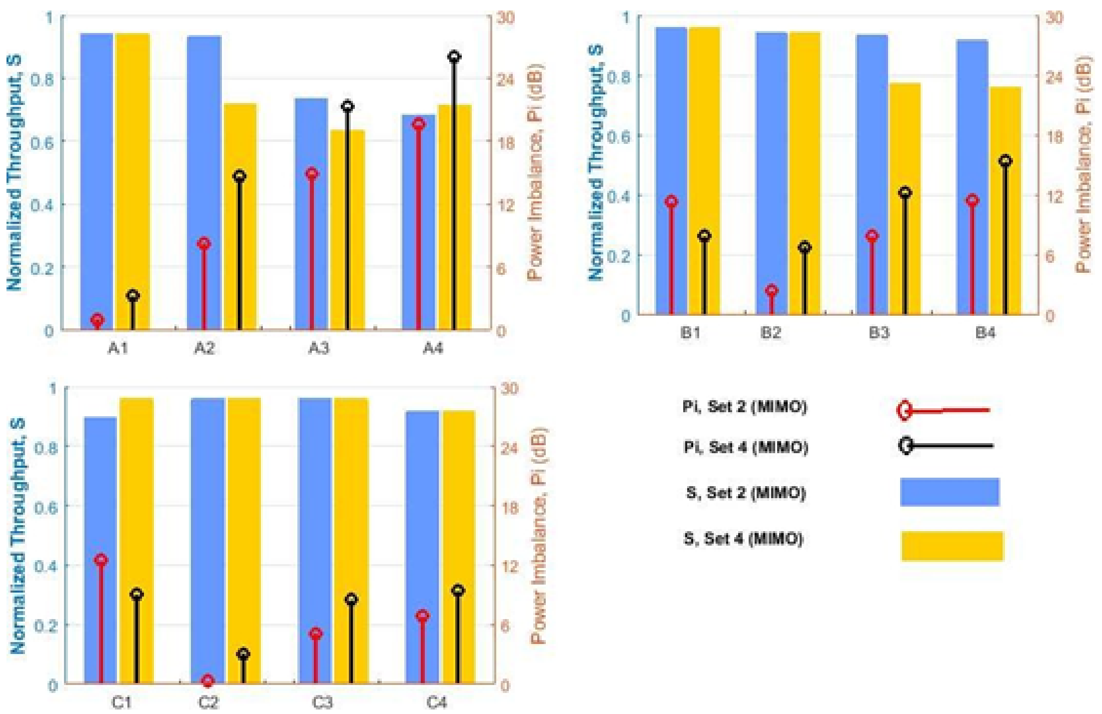


Figure 15: Throughput, as represented by S, represents power imbalance this computation gives the results of MIMO utilising sets 2 and 4.

Table 4: Experimental Results for set4 & set2

| | | Set 4 | | | | Set 2 | | | |
|---|---|---|---|---|---|---|---|---|---|
| | | 1 | 2 | 3 | 4 | 1 | 2 | 3 | 4 |
| Row A | Pi (dB) | 3.15 | 14.64 | 21.3 | 26.03 | -0.96 | 8.31 | 14.65 | 19.41 |
| | S | 0.942 | 0.72 | 0.654 | 0.712 | 0.938 | 0.944 | 0.754 | 0.62 |
| | Pr1(dBm) | -52.56 | -44.5 | -40.29 | -37.7 | -56.65 | -52 | -46.65 | -44.12 |
| | Pr2 (dBm) | -54.78 | -59.34 | -61.53 | -56.14 | -44.59 | -58.69 | -61.54 | -61.8 |
| Row B | Pi( dB ) | -7.849 | 6.74 | 12.15 | 15.41 | -11.31 | 2.38 | 7.9 | 11.45 |
| | S | 0.96 | 0.939 | 0.782 | 0.75 | 0.96 | 0.961 | 0.945 | 0.926 |
| | Pr1(dBm) | -54.12 | -48.79 | -47.22 | -46.41 | -57.1 | -53.65 | -51.123 | -50.16 |
| | Pr2(dBm) | -46.289 | -55.71 | -59.33 | -61.53 | -46.3 | -55.31 | -59.56 | -62.56 |
| Row C | Pi (dB) | -9.059 | 3.09 | 8.52 | 9.523 | -12.51 | -0.35 | 5.22 | 6.9 |
| | S | 0.957 | 0.96 | 0.956 | 0.917 | 0.91 | 0.96 | 0.96 | 0.912 |
| | Pr1(dBm) | -53.848 | -51.31 | -51.12 | -49.71 | -57.36 | -55.25 | -54.123 | -54.156 |
| | Pr2(dBm) | -44.78 | -54.34 | -58.53 | -59.14 | -44.59 | -54.69 | -58.54 | -59.8 |

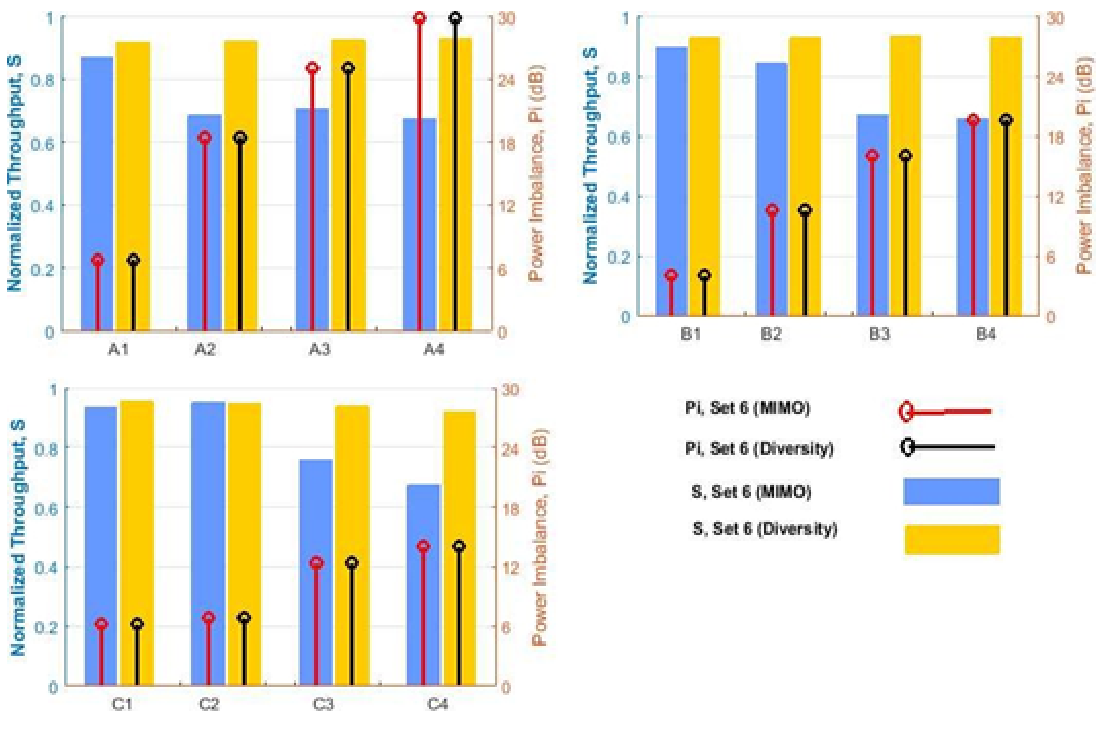


Figure 16: Throughput: the ability to produce and deliver results the set 6 MIMO Pi findings

throughput performance beyond 0.65 to 0.7, even as the imbalance problem grows. It can also be expressed as: It is as much as 30 dB in Position A4, but it is more even in Set 2, where the total throughput is around 0.67.

## 6 Conclusion

These concerns with commercial MIMO access points in DAS have been analyzed in this paper: namely, discrepancies in fiber length and power imbalances. To verify if there were performance advantages associated with deploying MIMO-enabled APs, we employed two types of MIMO-supported APs. When the fiber link difference (100m) increases, the transmission line throughput dramatically decreases. The 150m fiber link difference notwithstanding, the high throughputs were maintained despite the evidence of the poorer link reliability. One antenna port is transmitting alone, and that single antenna port is responsible for delivering information over time slots. To also find if there was a correlation between the DAS output performance and the amount of imbalance power, the throughput-received power was also investigated. Results show that when receiver sensitivity is exceeded by 12dB, throughput is significantly reduced. Lastly, it should be emphasized that the results of a wireless propagation model are not the same in a real environment. Additionally, no specific limit can be specified for the imbalance in power between a 2x2 MIMO systems. This result is in accordance with the LTE maximum acceptable range of (12 to 15) dB.

## References


[1] A. Al-fatlawia, M. A. Zahra, and H. Rassool, *Simulation of optical fiber cable regarding bandwidth limitations*, Int. J. Nonlinear Anal. Appl. **12** (2021), no. Special Issue, 1159–1174.

[2] P. Assimakopoulos, A. Nkansah, and N. Gomes, *Use of commercial access point employing spatial diversity in a distributed antenna network with different fiber lengths*, 2008 Int. Topical Meeting on Microwave Photonics Jointly held with the 2008 Asia-Pacific Microwave Photonics Conference, IEEE, 2008, pp. 189–192.

[3] H. Bölcskei, D. Gesbert, C. Papadias, and A. V. der Veen, *Space-time wireless systems: from array processing to mimo communications*, Cambridge University Press, 2006.

[4] T. Chrysikos, G. Georgopoulos, and S. Kotsopoulos, *Site-specific validation of itu indoor path loss model at 2.4 ghz*, 2009 IEEE International Symposium on a World of Wireless, Mobile and Multimedia Networks & Workshops, IEEE, 2009, pp. 1–6.

[5] M. Crisp, S. Li, A. Watts, R. Penty, and I. White, *Uplink and downlink coverage improvements of 802.11 g signals using a distributed antenna network*, J. Lightwave Technol. **25** (2007), no. 11, 3388–3395.

[6] G. Gordon, M. Crisp, R. Penty, and I. White, *Experimental evaluation of layout designs for 3×3 mimo-enabled radio-over-fiber distributed antenna systems*, IEEE Trans. Veh. Technol. **63** (2013), no. 2, 643–653.

[7] A. Hekkala, M. Lasanen, I. Harjula, L. Viera, N. Gomes, A. Nkansah, S. Bittner, F. Diehm, and V. Kotzsch, *Analysis of and compensation for non-ideal rof links in das [coordinated and distributed mimo]*, IEEE Wireless Commun. **17** (2010), 52–59.

[8] IEEE, *Std. 802.11g/d1.1-2001*, Part 11: Wireless LAN Medium Access Control (MAC) and Physical Layer (PHY) Specifications: Further Higher-Speed Physical Layer Extension in the 2.4 GHz band, 2003.

[9] C. Kim and J. Lee, *Dynamic rate-adaptive mimo mode switching between spatial multiplexing and diversity*, EURASIP J. Wireless Commun. Network. **2012** (2012), no. 1, 1–12.

[10] A. Kobyakov, D. Thelen, A. Chamarti, M. Sauer, and J. Winters, *Mimo radio signals over fiber in picocells for increased wlan coverage*, OFC/NFOEC 2008-2008 Conference on Optical Fiber Communication/National Fiber Optic Engineers Conference, IEEE, 2008, pp. 1–3.

[11] W. Lee, *Vertical vs. horizontal separations for diversity antennas*, Cellular Bus. (1991), 56–60, `http://www.commscope.com/docs/antenna_separation_article_ta`.

[12] Y. S. Mahmood and G. A. Qasmarrogy, *Capacity analysis of multiple-input-multiple-output system over rayleigh and rician fading channel*, Cihan Univ.-Erbil Sci. J. **3** (2019), no. 2, 70–74.

[13] M. Sauer and A. Kobyakov, *Fiber-radio antenna feeding for mimo systems*, Asia Optical Fiber Communication and Optoelectronic Exposition and Conference, Optical Society of America, 2008, p. SaJ6.

[14] M. Tolstrup, *ndoor radio planning: A practical guide for gsm, dcs, umts, hspa and lte*, vol. Second Edition, John Wiley & Sons, Inc., 2011.

[15] E. Vitucci, L. Tarlazzi, F. Fuschini, P. Faccin, and V. Degli-Esposti, *Interleaved-mimo das for indoor radio coverage: concept and performance assessment*, IEEE Trans. Antennas Propag. **62** (2014), no. 6, 3299–3309.

[16] T. Yamakami, T. Higashino, K. Tsukamoto, and S. Komaki, *An experimental investigation of applying mimo to rof ubiquitous antenna system*, 2008 International Topical Meeting on Microwave Photonics jointly held with the 2008 Asia-Pacific Microwave Photonics Conference, IEEE, 2008, pp. 201–204.

[17] K. Zhu, M. Crisp, S. He, R. Penty, and I. White, *Mimo system capacity improvements using radio-over-fibre distributed antenna system technology*, Optical Fiber Commun. Conf., Optical Society of America, 2011, pp. 1–3.